Spin Waves without Spin Waves: A Case for Soliton Propagation in Starling Flocks

Andrea Cavagna,[1,2,3] Guido Cimino,[2,1,*] Javier Cristín,[4] Matteo Fiorini,[2,1] Irene Giardina,[2,1,3] Angelo Giustiniani,[2,1] Tomás S. Grigera,[5,6,7,1] Stefania Melillo,[1,8] Roberto A. Palombella,[8,1] Leonardo Parisi,[1,8] Antonio Ponno,[9] Mattia Scandolo,[10] and Zachary S. Stamler[8,1]

[1]*Istituto Sistemi Complessi, Consiglio Nazionale delle Ricerche, UOS Sapienza, 00185 Rome, Italy*
[2]*Dipartimento di Fisica, Università Sapienza, 00185 Rome, Italy*
[3]*Istituto Nazionale di Fisica Nucleare, Sezione Roma 1, Rome, Italy*
[4]*Departament de Física, Universitat Autònoma de Barcelona, 08193 Bellaterra, Spain*
[5]*Instituto de Física de Líquidos y Sistemas Biológicos CONICET-Universidad Nacional de La Plata, La Plata, Argentina*
[6]*CCT CONICET La Plata, Consejo Nacional de Investigaciones Científicas y Técnicas, La Plata, Argentina*
[7]*Departamento de Física, Facultad de Ciencias Exactas, Universidad Nacional de La Plata, La Plata, Argentina*
[8]*Dipartimento di Fisica, Università Sapienza, 00185 Rome, Italy*
[9]*Dipartimento di Matematica T. Levi-Civita, Università degli Studi di Padova, 35131 Padova, Italy*
[10]*James Franck Institute, University of Chicago, 60637 Chicago, Illinois, USA*

(Received 28 August 2025; revised 28 January 2026; accepted 3 June 2026; published 27 August 2026)

Collective turns in starling flocks propagate linearly with negligible attenuation, indicating the existence of an underdamped sector in the dispersion relation. According to linear response theory, beside granting linear propagation of the phase perturbations, the real part of the frequency should also yield a spin-wave form of the unperturbed correlation function. However, new high-resolution experiments on real flocks show that underdamped traveling waves coexist with an overdamped Lorentzian correlation. Theory and experiments are reconciled once we add to the dynamics a Fermi-Pasta-Ulam-Tsingou term.

DOI: 10.1103/sppm-qsnb

Experiments on starling flocks [1] show that collective turns propagate across the group as linear waves with very little damping (Videos S1 and S2 [2]) and with a speed of propagation that is higher the larger the polarization; these waves are not accompanied by significant density fluctuations, as the interaction network remains nearly unchanged during the turn. Moreover, birds turn along equal-radius—rather than parallel—trajectories, which allows them to keep their speed within a physiological range [26]. To explain this phenomenology the inertial spin model (ISM) was introduced in [1,27]: at equilibrium the ISM belongs to Model G universality class [28], hence its low temperature phase sustains phase waves (second sound) even in absence of density fluctuations (first sound). In the ISM the velocity $\mathbf{v}_i$ is turned by the spin $\mathbf{s}_i$, which is the generator of the rotations in the internal space of the velocity, while the spin is acted upon by the social alignment force,

$$\begin{aligned}\dot{\mathbf{v}}_i &= \frac{\partial H}{\partial \mathbf{s}_i} \times \mathbf{v}_i, \\ \dot{\mathbf{s}}_i &= -\mathbf{v}_i \times \frac{\partial H}{\partial \mathbf{v}_i} - \frac{\eta}{\chi}\mathbf{s}_i + \boldsymbol{\xi}_i,\end{aligned} \tag{1}$$

where the pseudo-Hamiltonian is given by

$$H = \sum_i \frac{\mathbf{s}_i^2}{2\chi} + \frac{J_2}{4v_0^2}\sum_{ij} n_{ij}(\mathbf{v}_i - \mathbf{v}_j)^2. \tag{2}$$

From a geometrical point of view, the spin is proportional to the curvature of the trajectory [1,27]: when a bird is flying straight its spin is zero; the interaction with other birds can produce a force that increases the spin, thus generating a nonzero curvature, and thus a change of heading. This mechanism restores the inertial dynamics of directional changes. The adjacency matrix n_{ij} depends on time due to the self-propulsion equation, $\dot{\mathbf{r}}_i = \mathbf{v}_i$ (whence "pseudo" Hamiltonian); the noise has correlator $\langle \xi_i^\mu(t)\xi_j^\nu(t')\rangle = 2\eta T\delta(t-t')\delta_{ij}\delta^{\mu\nu}$, and the velocity modulus is fixed, $|\mathbf{v}_i| = v_0$. The parameter J_2 is the alignment coupling constant (or stiffness), while χ is the (generalized) inertia and η is the nonconservative friction. The ISM's overdamped limit is the Vicsek model [29]. In the low-temperature symmetry-broken phase the velocities predominantly point in the same mean direction,

*Contact author: gu.cimino@uniroma1.it

$\mathbf{v} = (1/N)\sum_i \mathbf{v}_i$, hence we can expand in the small transverse fluctuations, $\boldsymbol{\pi}_i$, writing, $\mathbf{v}_i = \mathbf{v}_i^L + \boldsymbol{\pi}_i$, where $\mathbf{v}_i^L$ are the longitudinal components, satisfying the relation $|\mathbf{v}_i^L| = \sqrt{v_0^2 - \boldsymbol{\pi}_i^2}$, and where $|\boldsymbol{\pi}_i| \ll |\mathbf{v}_i|$, with $\boldsymbol{\pi}_i \cdot \mathbf{v}_i = 0$ [30]. By expanding linearly in $\boldsymbol{\pi}_i$ the homogeneous equation of motion for the velocity [see Supplemental Material (SM) [2]] we obtain

$$\chi\ddot{\boldsymbol{\pi}}_i + \eta\dot{\boldsymbol{\pi}}_i + J_2\sum_j \Lambda_{ij}\boldsymbol{\pi}_j = 0, \tag{3}$$

where $\Lambda_{ij} = -n_{ij} + \delta_{ij}\sum_k n_{ik}$ is the discrete Laplacian. By assuming that $n_{ij}(t)$ varies slowly compared to the velocity's relaxation time [31] and by going to the continuum limit, $J_2\Lambda_{ij} \to -J_2 n_c r_1^2 \nabla^2$ (where r_1 is the mean interparticle distance and n_c is the mean number of interacting neighbors), we can derive the quasiequilibrium dispersion relation of the ISM,

$$\omega(k) = -i\gamma \pm \sqrt{(J_2 n_c/\chi) r_1^2 k^2 - \gamma^2}; \qquad \gamma = \eta/2\chi. \tag{4}$$

In the underdamped regime, $(J_2 n_c/\chi) r_1^2 k^2 \gg \gamma^2$, the real part of the frequency becomes, $\omega(k) \approx \pm c_s k$, with $c_s = r_1\sqrt{J_2 n_c/\chi}$; hence, the system sustains linearly propagating waves with speed c_s.

Simulations performed in the active case, namely with a dynamically evolving adjacency matrix $n_{ij}(t)$, confirm the quasiequilibrium framework above: within the deeply underdamped phase, a perturbation that changes the direction of a single particle—the initiator—propagates through the entire group, eliciting a collective turn (Fig. 1; the precise turning protocol is reported in SM [2]). On the other hand, in the overdamped phase, $(J_2 n_c/\chi) r_1^2 k^2 < \gamma^2$, damping and sublinear diffusion dominate. In these conditions it is not possible to have the flock make a *realistic* turn: either the flock disintegrates (Fig. 1), or it fails to meet the quantitative criteria that characterize biologically plausible turns in real experiments (see End Matter and Videos S4–S7 [2]). The speed of propagation of the turn in real flocks was found to be in line with the ISM prediction: in the ordered phase the polarization $\Phi = |\mathbf{v}|/v_0$, is connected to the transverse fluctuations by $(1-\Phi) \approx \langle \boldsymbol{\pi}^2/v_0^2\rangle/2 \sim T/J_2$ (prefactors depend on lattice details [30,32,33]), so that $c_s \sim 1/\sqrt{1-\Phi}$, a prediction in fair agreement with experiments [1].

The existence of a real part of the frequency in the underdamped regime has another consequence. Linear response theory predicts that the spectrum of the response determines also the spectrum of the spontaneous fluctuations. Hence the correlation function of the velocity fluctuations displays two spin-wave (SW) peaks at $\omega_{\mathrm{sw}} = \pm c_s k$; conversely, in the overdamped phase, $c_s^2 k^2 < \gamma^2$, the correlation function is quasi-Lorentzian (L), with full width at half-maximum frequency,

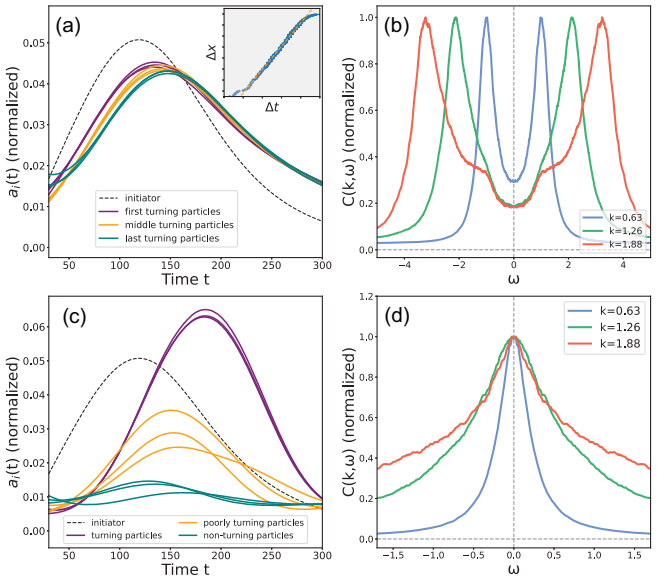

FIG. 1. Simulations—ISM. Upper panels: underdamped regime. (a) The velocity of the initiator is rotated by $\pi/2$; the accelerations of all the particles show coherent turning, with little damping (Video S3 [2]). Inset: the distance traveled by the perturbation (extracted from the maxima of the accelerations; see SM [2]), is linear in the time elapsed since the initiator's turn. (b) The unperturbed velocity correlation function has clear spin-wave peaks at $\omega_{SW} = \pm c_s k$. Lower panels: overdamped regime. (c) No collective turn: the acceleration curves show that not all individuals can follow the initiator (Video S4 [2]). (d) The velocity correlation function is Lorentzian, with characteristic frequency $\omega_L \sim k^2$. Simulations are performed in $d = 3$ with a dynamically evolving adjacency matrix $n_{ij}(t)$ (self-propelled particles). To compare simulations with experiments, accelerations are normalized by the scale v_0^2/r_1. Simulation parameters are specified in SM [2].

$\omega_{\mathrm{L}} = (J_2 n_c/\eta) r_1^2 k^2$. In SM [2] we perform a linear analysis of the out-of-equilibrium active field theory corresponding to (1), in which $n_{ij}(t)$ is *not* assumed to be constant, hence including density fluctuations, and show that also the active case conforms to this spin-wave phenomenology. Simulations of the ISM confirm this scenario (Fig. 1). Note that the association of spin-wave peaks and traveling waves does not depend on the specific way propagating modes emerge, whether it is through inertia, as in the ISM, or through the velocity-density coupling giving rise to first sound, as in Toner-Tu's theory [34–36]: whenever the frequency develops a real part, there should be both sound propagation and sound peaks.

Experimental evidence on starling flocks starkly disagrees with this scenario, though. To compute the correlation functions accurately enough to resolve the potential spin-wave peaks one needs a small frequency step, which requires experimental acquisitions with time duration significantly longer than those of [1]. To this end, we developed a new panning 3D stereo system and conducted

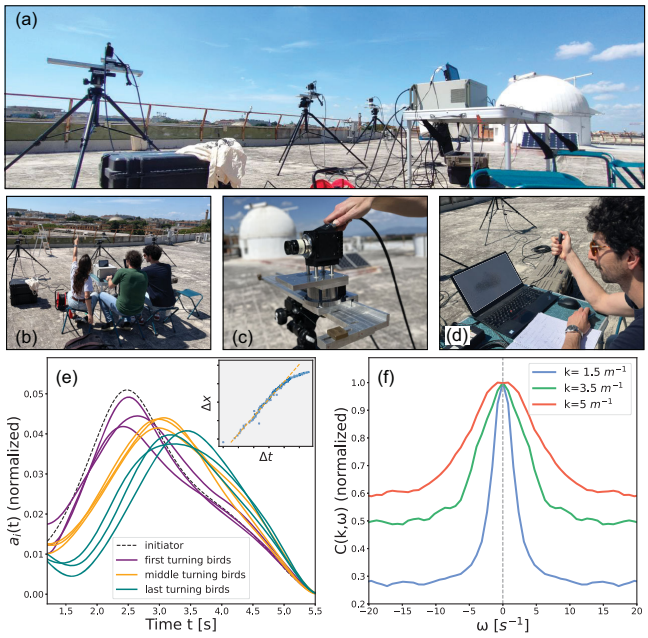

FIG. 2. Experiments—starling flocks. (a)–(d) In the new experimental setup micrometric rotors (c) are used to pan the stereo camera system and track flocks for longer time intervals (up to 12.5 s vs 3 s of the old experiments, SM [2]). (e) In turning flocks phase perturbations propagate linearly with negligible dissipation, as in the underdamped phase of the ISM [Fig. 1(a)], and yet (f) the correlation function measured during straight flight has a quasi-Lorentzian form: there are no spin-wave peaks, as in the overdamped phase of the ISM [Fig. 1(d)]. See SM [2] for the criteria used to separate straight flights from turns.

new experiments that we present here for the first time [Figs. 2(a)–2(d) and SM [2]): thanks to the longer acquisitions, we are able not only to measure the dynamics of turns, but also the spectrum of *spontaneous* fluctuations, which we define as the birds' small changes of direction in flocks that follow a straight path (for the definition of turning vs straight flights, see SM [2]). On the other hand, we interpret the anomalously large phase fluctuation of a few individuals that precede a global change of direction as the result of an external *perturbation*; admittedly, although turns can be plausibly caused by external influences such as predators, these sources are outside the field of view of the experimental acquisitions and thus cannot be unambiguously identified. Therefore, when we say "perturbations" in experiments, strictly speaking we mean anomalous local fluctuations, able to trigger a global change of direction. Surprisingly, the correlation functions measured during straight flight from this new dataset [Fig. 2(f) and SM [2]] do not show any evidence of spin-wave peaks; instead, they display a Lorentzian-like central peak at $\omega = 0$, with full width at half-maximum $\omega_L \sim k^2$ (SM [2]), both clear hallmarks of an overdamped system. And yet, phase perturbations *do* propagate linearly across the group, eliciting collective turns [Fig. 2(e)]. So, starling flocks develop traveling spin waves under perturbation, without spin waves in the spectrum of spontaneous fluctuations. How is that possible?

There are two potential ways out of this paradox: either some further out-of-equilibrium effect radically changes the spin-wave prediction; or the relationship between response to a perturbation and unperturbed correlation is not the one we expected. The first hypothesis is unlikely, as the inclusion of out-of-equilibrium density fluctuations in the theory at the linear level does not change the classic spin-wave scenario (SM [2]) and simulations thoroughly confirm that. The second possibility seems absurd as long as we stay within the boundaries of linear response theory. But, if a strong nonlinearity is present, then things can change—even at equilibrium.

The strong polarization of bird flocks is due to the fact that spontaneous phase fluctuations are weak; on the other hand, a localized phase distortion due to a perturbation—and in particular one able to elicit a collective turn—may be much stronger: flocks typically turn because some individual perceives an external threat, hence changing heading in a robust way compared to its normal cruising fluctuations. A possible way to make progress, then, is to hypothesize that individuals respond weakly to small fluctuations in the orientation of their neighbors—which are perceived as normal business—and very strongly to large phase distortions, which may signal a threat. This would imply that the stiffness, i.e., the alignment coupling constant, is not in fact a constant, but increases when the local phase distortion $\delta\varphi$ increases. In this way, due to their small stiffness, spontaneous fluctuations would be overdamped, showing no spin-wave peaks in the correlation function, while when a perturbation causes a large distortion in the local phase, the stiffness suddenly increases and the system becomes underdamped, therefore able to propagate the phase wave necessary for the flock to collectively turn.

We choose the simplest way to implement this mechanism, namely to introduce a nonquadratic term in the $\mathbf{v}$-dependent part of the Hamiltonian

$$H_{\mathbf{v}} = \frac{J_2}{4v_0^2}\sum_{ij} n_{ij}(\mathbf{v}_i - \mathbf{v}_j)^2 + \frac{J_4}{4v_0^4}\sum_{ij} n_{ij}(\mathbf{v}_i - \mathbf{v}_j)^4, \quad (5)$$

where we have used a Landau approach, simply including the next nontrivial term in the potential expansion (better avoiding the RG-loaded word "relevant" in this low-T context). As we shall see, this is enough to reproduce current experimental observations, but of course we cannot exclude that future experiments may require higher order terms to match theory and experiments.

For the sake of the following arguments it is convenient to consider planar velocities, hence transverse fluctuations $\boldsymbol{\pi}_i$ become scalars and we can expand (5) in the dimensionless phases, $\varphi_i = \pi_i/v_0$, to obtain (see SM [2])

$$H_{\mathbf{v}} \approx \frac{1}{4}\sum_{ij} n_{ij}(\varphi_i - \varphi_j)^2[J_2 + J_4(\varphi_i - \varphi_j)^2], \quad (6)$$

which naturally invites us to define an effective stiffness,

$$J_{\text{eff}} = J_2 + J_4\delta\varphi^2. \quad (7)$$

Relation (7) aligns with our theoretical idea of having a stiffness that sharply increases with the local phase distortion. But can we find a sector in the parameter space in which this mechanism actually works?

First of all, we require that spontaneous phase fluctuations, $\delta\varphi^2_{\text{spnt}}$, are ruled by J_2, while much larger phase distortions due to external perturbations, $\delta\varphi^2_{\text{pert}} \gg \delta\varphi^2_{\text{spnt}}$, are ruled by J_4; we see from (7) that this amounts to requiring, $J_4\delta\varphi^2_{\text{spnt}} \ll J_2 \ll J_4\delta\varphi^2_{\text{pert}}$. Secondly, to produce Lorentzian correlation of spontaneous fluctuations, J_2 must be *overdamped*, while large phase distortions ruled by J_4 must be *underdamped* to propagate; relation (4) shows that the effective overdamping scale of a system with size L is $\gamma_L^2 \equiv \gamma^2 L^2\chi/(4\pi^2 n_c r_1^2)$, hence we need $J_2 \ll \gamma_L^2 \ll J_4\delta\varphi^2_{\text{pert}}$. We can rearrange these requirements in the following way,

$$J_4\delta\varphi^2_{\text{spnt}} \ll J_2 \ll \gamma_L^2 \ll J_4\delta\varphi^2_{\text{pert}}. \quad (8)$$

Simply stated, J_2 must be overdamped, while J_4 must be small enough to remain dormant under spontaneous phase fluctuations, but large enough to rule the transport of large phase distorsions. Spontaneous phase fluctuations are connected to the polarization by the relation $\delta\varphi^2_{\text{spnt}} \approx 2(1-\Phi)$, hence they are very small in the deeply ordered regime flocks belong to; hence, it is not hard to envisage perturbations yielding $\delta\varphi^2_{\text{pert}} \gg \delta\varphi^2_{\text{spnt}}$, which leaves the necessary margin to satisfy (8).

Numerical simulations of (1)–(5) in the general $3d$ nonplanar, active case confirm this theoretical scenario (Fig. 3).

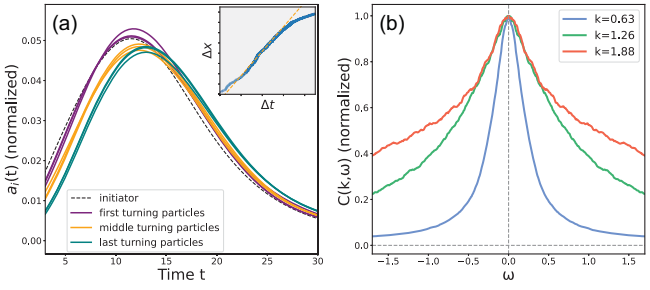

FIG. 3. Simulations—ISM with quartic interaction. (a) When a quartic term is added to the interaction, linear underdamped propagation of phase perturbations is achieved (Video S8 [2]), and (b) the spectrum of spontaneous fluctuations remains Lorentzian (overdamped), as in natural flocks (Fig. 2). Simulations are performed in $d = 3$. Simulation parameters are specified in SM [2].

When the polarization is high, the quadratic stiffness J_2 is low and the nonlinear coupling J_4 is large, the new model gives the same phenomenology as in real experiments: in absence of external perturbations we find a Lorentzian correlation function, with half-maximum width $\omega_{\text{L}} \sim k^2$ (SM); at the same time, when one individual turns, there is linear wave propagation, eliciting a collective turn of the entire group (Fig. 3 and Video S8). Spontaneous fluctuations, ruled by the low stiffness J_2, are overdamped, while external perturbations respond to the large nonlinear stiffness J_4, which makes them underdamped (the numerical robustness of this scenario is discussed in details in Appendix B). We also note that the relation $(1-\Phi) \approx \langle \boldsymbol{\pi}^2/v_0^2\rangle/2$, depends only on the expansion for small $\boldsymbol{\pi}_i$, hence if we extend to J_{eff} the standard low-T relations, $\langle \boldsymbol{\pi}^2/v_0^2\rangle \sim T/J_{\text{eff}}$ and $c_s \sim \sqrt{J_{\text{eff}}}$, we obtain the same prediction as in the standard ISM for how the speed of propagation should depend on the polarization during turn propagation, $c_s \sim 1/\sqrt{1-\Phi}$, which is well verified by experiments on real flocks [1]. Finally, we prove in SM [2] that the new model works fine also with fluctuating speeds and in the case of small changes of direction of the entire group, provided that they are larger than the spontaneous phase fluctuations.

When we explicitly write down the equations of motion for the planar phases φ_i in the new model (see SM [2]), and neglect both noise and dissipation, we obtain evolution equations identical in form to those of the Fermi-Pasta-Ulam-Tsingou (FPUT) model [37,38],

$$\ddot{\varphi}_i + \sum_j n_{ij}(\varphi_i - \varphi_j) + 2\frac{J_4}{J_2}\sum_j n_{ij}(\varphi_i - \varphi_j)^3 = 0. \quad (9)$$

These equations are, up to a time rescaling $t \to \sqrt{J_2/\chi}t$, the equations associated to the Hamiltonian $H(\varphi, s) = [1/(2\chi)]\sum_i s_i^2 + H_{\mathbf{v}}$, where the "potential" energy $H_{\mathbf{v}}$ is given by (6). A well-known property of the FPUT dynamics is that the competition between nonlinearity and dispersion, ruled by the ratio J_4/J_2, allows for the propagation of solitary waves, or *solitons*, in both one and two dimensional lattices [39–41]. Although the problem at hand requires on to consider FPUT solitons on an adiabatically evolving $3d$ interaction network—to take into account activity—and to consider the theoretical effects of weak noise [42] and dissipation [43] on the general FPUT mechanism, it is very tempting to interpret the traveling waves that we obtain in the new model—and that we observe in natural flocks—as FPUT solitons.

Our theoretical arguments are based on infinite-sized systems, whereas natural flocks have finite size; in particular, the reduction of the coordination number near the edges may affect signal propagation. Due to the highly irregular shapes of natural flocks, it is very hard—if not impossible—to formulate a theoretical prediction for this

effect. However, we note that also the numerical turning flocks analyzed here have edges, so that—even though we cannot reproduce the highly diverse shapes of experimental flocks—the effect of reduction of the coordination number is present in simulations as well as in experiments. Hence, the fact that simulations of the ISM-FPUT model correctly reproduce the experimental observables indicates that edge effects are not strong enough to hinder the theoretical scenario to the extent of invalidating its main predictions.

In conclusion, we have conducted new experiments on starling flocks, finding a puzzling phenomenology: large disturbances of the phase are linearly transported, giving rise to collective turns, while spontaneous phase fluctuations are overdamped, producing a Lorentzian correlation function with no evidence of the standard spin-wave peaks that normally accompany traveling waves. The ISM, originally introduced to account for underdamped linear propagation, cannot explain an overdamped correlation function. To reconcile experiments with theory we have added a quartic term to the alignment interaction, thanks to which weak spontaneous fluctuations of the phase are overdamped, while finite phase perturbations are underdamped, and therefore propagate linearly. The power unit of the new dynamics is a FPUT core, suggesting that directional information within natural flocks of starlings is transported by nonlinear solitary waves.

Acknowledgments—We thank William Bialek, Enzo Branchini, Fabio Cecconi, Giulio Costantini, Viktor Holubec, and Mario Veca for insightful discussions. This work was supported by ERC Grant RG.BIO (Contract No. 785932), MIUR Grant INFO.BIO (Protocol No. R18JNYYMEY), and MIUR Grant PRIN2020 (Contract No. 2020PFCXPE-005).

Data availability—There are no publicly available research data or software supporting this manuscript. Requests for further information or data should be sent to the authors.

[1] A. Attanasi, A. Cavagna, L. Del Castello, I. Giardina, T. S. Grigera, A. Jelić, S. Melillo, L. Parisi, O. Pohl, E. Shen *et al.*, Nat. Phys. **10**, 691 (2014).
[2] See Supplemental Material at http://link.aps.org/supplemental/10.1103/sppm-qsnb for experimental details, theoretical calculations, and additional simulations. Includes Refs. [3–25].
[3] A. Cavagna, X. Feng, S. Melillo, L. Parisi, L. Postiglione, and P. Villegas, IEEE Trans. Instrum. Meas. **70**, 1 (2021).
[4] A. Attanasi, A. Cavagna, L. Del Castello, I. Giardina, A. Jelić, S. Melillo, L. Parisi, F. Pellacini, E. Shen, E. Silvestri *et al.*, IEEE Trans. Pattern Anal. Mach. Intell. **37**, 2451 (2015).
[5] A. Cavagna, I. Giardina, and T. S. Grigera, Phys. Rep. **728**, 1 (2018).
[6] A. Cavagna, J. Cristín, I. Giardina, T. S. Grigera, and M. Veca, J. Phys. A **57**, 415002 (2024).
[7] M. P. Allen and D. J. Tildesley, *Computer Simulation of Liquids* (Clarendon Press, Oxford, 1987).
[8] W. C. Swope, H. C. Andersen, P. H. Berens, and K. R. Wilson, J. Chem. Phys. **76**, 637 (1982).
[9] A. Cavagna, L. Di Carlo, I. Giardina, T. S. Grigera, S. Melillo, L. Parisi, G. Pisegna, and M. Scandolo, Nat. Phys. **19**, 1043 (2023).
[10] O. Chepizhko, D. Saintillan, and F. Peruani, Soft Matter **17**, 3113 (2021).
[11] Andrea, A. Cimarelli, I. Giardina, G. Parisi, R. Santagati, F. Stefanini, and M. Viale, Proc. Natl. Acad. Sci. U.S.A. **107**, 11865 (2010).
[12] A. Cavagna, A. Culla, X. Feng, I. Giardina, T. S. Grigera, W. Kion-Crosby, S. Melillo, G. Pisegna, L. Postiglione, and P. Villegas, Nat. Commun. **13**, 2315 (2022).
[13] W. Bialek, A. Cavagna, I. Giardina, T. Mora, O. Pohl, E. Silvestri, M. Viale, and A. M. Walczak, Proc. Natl. Acad. Sci. U.S.A. **111**, 7212 (2014).
[14] A. Cavagna, A. Culla, L. Di Carlo, I. Giardina, and T. S. Grigera, C.R. Phys. **20**, 319 (2019).
[15] A. Cavagna, A. Culla, and T. S. Grigera, Phys. Rev. E **106**, 054136 (2022).
[16] A. Cavagna, L. Di Carlo, I. Giardina, T. S. Grigera, and G. Pisegna, Phys. Rev. Res. **3**, 013210 (2021).
[17] J. Zinn-Justin, *Quantum Field Theory and Critical Phenomena*, 4th ed., International Series of Monographs on Physics Vol. 113 (, Oxford, England, 2002), pp. 1054.
[18] A. Cavagna, I. Giardina, T. S. Grigera, A. Jelic, D. Levine, S. Ramaswamy, and M. Viale, Phys. Rev. Lett. **114**, 218101 (2015).
[19] A. Cavagna, L. Di Carlo, I. Giardina, L. Grandinetti, T. S. Grigera, and G. Pisegna, Phys. Rev. E **100**, 062130 (2019).
[20] A. Cavagna, L. Di Carlo, I. Giardina, L. Grandinetti, T. S. Grigera, and G. Pisegna, Phys. Rev. Lett. **123**, 268001 (2019).
[21] Y. Tu, J. Toner, and M. Ulm, Phys. Rev. Lett. **80**, 4819 (1998).
[22] L. H. Ryder, *Quantum Field Theory* (Cambridge University Press, Cambridge, England, 1996).
[23] A. Z. Patashinskii and V. L. Pokrovskii, Zh. Eksp. Teor. Fiz. **64**, 1445 (1973).
[24] A. Z. Patashinskii and V. L. Pokrovskii, *Fluctuation Theory of Phase Transitions* (Pergamon Press, New York, 1979).
[25] A. Attanasi, A. Cavagna, L. Del Castello, I. Giardina, A. Jelic, S. Melillo, L. Parisi, O. Pohl, E. Shen, and M. Viale, J. R. Soc. Interface **12**, 20150319 (2015).
[26] H. Pomeroy and F. Heppner, The Auk **109**, 256 (1992).
[27] A. Cavagna, L. Del Castello, I. Giardina, T. Grigera, A. Jelic, S. Melillo, T. Mora, L. Parisi, E. Silvestri, M. Viale *et al.*, J. Stat. Phys. **158**, 601 (2015).
[28] P. C. Hohenberg and B. I. Halperin, Rev. Mod. Phys. **49**, 435 (1977).
[29] T. Vicsek, A. Czirók, E. Ben-Jacob, I. Cohen, and O. Shochet, Phys. Rev. Lett. **75**, 1226 (1995).
[30] F. Dyson, Phys. Rev. **102**, 1217 (1956).
[31] T. Mora, A. M. Walczak, L. Del Castello, F. Ginelli, S. Melillo, L. Parisi, M. Viale, A. Cavagna, and I. Giardina, Nat. Phys. **12**, 1153 (2016).

[32] W. Bialek, A. Cavagna, I. Giardina, T. Mora, E. Silvestri, M. Viale, and A. M. Walczak, Proc. Natl. Acad. Sci. U.S.A. **109**, 4786 (2012).
[33] A. Cavagna, D. Conti, I. Giardina, T. S. Grigera, S. Melillo, and M. Viale, Phys. Biol. **13**, 065001 (2016).
[34] J. Toner and Y. Tu, Phys. Rev. Lett. **75**, 4326 (1995).
[35] Y. Tu, J. Toner, and M. Ulm, Phys. Rev. Lett. **80**, 4819 (1998).
[36] J. Toner and Y. Tu, Phys. Rev. E **58**, 4828 (1998).
[37] E. Fermi, P. Pasta, S. Ulam, and M. Tsingou, Studies of the nonlinear problems, Technical Report, Los Alamos National Laboratory (LANL), Los Alamos, NM (USA), 1955.
[38] G. Gallavotti, *The Fermi-Pasta-Ulam Problem: A Status Report* (Springer, New York, 2008), Vol. 728.
[39] G. Friesecke and J. A. Wattis, Commun. Math. Phys. **161**, 391 (1994).
[40] G. Friesecke and K. Matthies, Discrete Contin. Dyn. Syst. B **3**, 105 (2003).
[41] F. Chen and M. Herrmann, Discrete Contin. Dyn. Syst. **38**, 2305 (2018).
[42] A. Orlowski and K. Sobczyk, Rep. Math. Phys. **27**, 59 (1989).
[43] H.-G. Purwins, H. Bödeker, and S. A. and, Adv. Phys. **59**, 485 (2010).
[44] H. Pomeroy and F. Heppner, Anim. Behav. **25**, 720 (1977).
[45] M. Ballerini, N. Cabibbo, R. Candelier, A. Cavagna, E. Cisbani, I. Giardina, V. Lecomte, A. Orlandi, G. Parisi, A. Procaccini *et al.*, Proc. Natl. Acad. Sci. U.S.A. **105**, 1232 (2008).
[46] D. Geiß, K. Kroy, and V. Holubec, Phys. Rev. E **106**, 054612 (2022).

End Matter

Appendix A: How to characterize biologically plausible turns—In the main text we have focused on the most conspicuous observables of flocking, namely linear propagation and cohesion during turns, together with Lorentzian correlation function during unperturbed flight. However, there is much more than this going on during a collective turn at the dynamic level, and the reader may ask whether we can characterize the phenomenon at a more detailed biological level. As a matter of fact we can, and this is important for testing the robustness of our new theory, as well as for ruling out other possible theories. The extra quantitative constraints that we use to select the correct dynamics involve two time scales, which can be directly measured in experiments and simulations alike: the first is the time employed by an individual bird to complete a turn and the second is the local relaxation time.

We define the duration of an individual turn, $\tau_{\rm turn}$, as the full-width at half-maximum of the curve of the centripetal acceleration of the initiator, i.e., of the first bird to turn; because we also require the whole group to maintain cohesion, the turning scale for all other birds will be similar to that of the initiator. The value of $\tau_{\rm turn}$ is an important experimental information; since birds cannot simply rotate without any spatial displacement, this parameter must be constrained by biomechanical traits. An average over 11 turning flocks yields $\tau_{\rm turn} = 2.3 \pm 0.3$ s, in experiments on starlings.

Second, we consider the relaxation time of the velocity fluctuations, measured at a local length scale. It is crucial to use a definition that measures the correlation of fluctuations at the *local* scale: the reason is that the *collective* relaxation time grows with the size of the system (because of the Goldstone mode due to the spontaneous breaking of the rotational symmetry); hence, the collective relaxation time does not constrain the model parameters: provided the system is ordered, one can get any desired collective relaxation time by changing the system's size. The relaxation time over scale $1/k$ for a Lorentzian correlation function, is given by $\tau_{\rm relax} = 2/\omega_{\rm L}(k)$, where $\omega_{\rm L}(k)$ is the full-width at half-maximum frequency of the Lorentzian peak. In order to have a local relaxation time, we evaluate the correlation at wavelength, $k_{\rm loc} = 2\pi/(2r_1)$, where r_1 is the nearest neighbor distance; the prefactor of r_1 used in this definition is not important, provided that it is the same in experiments and in simulations (more details and flock-by-flock measurements can be found in SM [2]). The experimental value, averaged over nine straight-flying flocks, is $\tau_{\rm relax} = 0.17 \pm 0.01$ s (this is perfectly consistent with previous determinations through dynamical inference, which give $\tau_{\rm relax} = 0.166$ s [31]).

In order to meaningfully compare experiments with simulations, we must normalize these two timescales through a "microscopic" temporal scale, so to produce dimensionless ratios. To do this we use the motility time, $\tau_{\rm mot}$, defined as the time needed for an individual to fly over a distance r_1, i.e., $\tau_{\rm mot} = r_1/v_0$, where v_0 is the mean birds' speed. For starlings we have $v_0 = 13 \pm 1$ m/s and $r_1 = 0.95 \pm 0.07$ m, so that the motility time is $\tau_{\rm mot} = 0.074 \pm 0.006$ s (interestingly the mean reaction time of starlings is 0.076 s to light stimuli, and 0.081 s to sound stimuli [44]). To summarize, the normalized experimental timescales that characterize biologically plausible turns are

$$\tau_{\rm relax}/\tau_{\rm mot} = 2.6 \pm 0.3, \qquad \tau_{\rm turn}/\tau_{\rm mot} = 28 \pm 2. \quad \text{(A1)}$$

It follows that any flocking model must be able to reproduce a Lorentzian correlation function, cohesive turns under perturbation, and finally it must reproduce both the dimensionless time scales (A1) to be acceptable.

Appendix B: Robustness of the ISM-FPUT scenario—There are ten parameters in the ISM-FPUT model: $\{J_2, J_4, \eta, v_0, \tau_{\rm turn}, T, L, r_1, \chi, n_c\}$. How much fine-tuning

do we need to meet all the experimental constraints? As we shall demonstrate here, not much. First, let us keep fixed the four parameters $\{L, r_1, \chi, n_c\}$: the flock size L and the nearest neighbor distance r_1 are quantities that vary significantly from flock to flock, hence they must be left free to take the values "they" want; the inertia χ can always be rescaled away in the equations, while the number of interacting neighbors, n_c, is an independent parameter which has been measured to be of order 10 in several past works [32,45]. So, we will assume that in a simulations these four parameters are fixed beyond our control, while we can choose $\{J_2, J_4, \eta, v_0, \tau_{\text{turn}}, T\}$ to produce numerical simulations that comply to the biological constraints.

The requirements we must meet to deem a turn biologically plausible are the following: the two dimensionless time scales (A1) must be matched, at least approximately; moreover, the flock must remain cohesive during the turn; i.e., the number of connected components, N_{conn}, must be one; finally, the unperturbed correlation function must be Lorentzian. We have seen in the main text that—within the ISM-FPUT model—the last two conditions are granted once the following relation is satisfied:

$$J_4\delta\varphi^2_{\text{spnt}} \ll J_2 \ll \gamma_L^2 \ll J_4\delta\varphi^2_{\text{pert}}. \tag{B1}$$

Let us use J_2 as an anchor in this chain of inequalities and fix it at an arbitrary value. In order to overdamp the spontaneous fluctuations ruled by J_2 we need to choose $\gamma_L^2 \gg J_2$; given that $\gamma_L^2 \sim \eta^2$, this condition requires that when we change J_2 the friction must compensate as, $\eta \sim J_2^{1/2}$ (here and in the following we disregard all constant parameters). From J_2 and η we can calculate the local relaxation time, $\tau_{\text{relax}} \sim \eta/J_2 \sim 1/J_2^{1/2}$, and then fix v_0 such that $\tau_{\text{relax}}/\tau_{\text{mot}} = 2.6$ (remember that $\tau_{\text{mot}} \sim 1/v_0$). Given that now τ_{mot} is fixed, we can choose τ_{turn} in such a way to have $\tau_{\text{turn}}/\tau_{\text{mot}} = 28$, hence fulfilling both relations (A1); note that this implies, $\tau_{\text{turn}} \sim 1/J_2^{1/2}$. Having closed the turning protocol through τ_{turn}, we must now choose J_4 in such a way that the term $J_4\delta\varphi^2_{\text{pert}}$ is much larger than γ_L^2, to verify the right inequality in (B1); but how does $J_4\delta\varphi^2_{\text{pert}}$ scale? A crude estimate can be given by equating potential and kinetic energy during the phase perturbation, $J_4\delta\varphi^4_{\text{pert}} \sim \dot{\varphi}^2$; because $\dot{\varphi}^2 \sim \tau_{\text{turn}}^{-2}$, we obtain, $\delta\varphi^2_{\text{pert}} \sim J_4^{-1/2}\tau_{\text{turn}}^{-1}$, and therefore, $J_4\delta\varphi^2_{\text{pert}} \sim J_4^{1/2}\tau_{\text{turn}}^{-1}$. To verify this argument we can directly measure $\delta\varphi^2_{\text{pert}}$ in simulations as the maximum phase distortion between the initiator and its nearest neighbors during the turn; the Pearson correlation coefficient (in log-log) between the numerical measurement of $J_4\delta\varphi^2_{\text{pert}}$ and its theoretical estimate, $J_4^{1/2}\tau_{\text{turn}}^{-1}$, is $R = 0.994$; therefore, the estimate is rather good and we can use it to choose J_4 in such a way to have $J_4\delta\varphi^2_{\text{pert}} \gg \gamma_L^2$. The last biological condition we need to impose is that $J_4\delta\varphi^2_{\text{spnt}} \ll J_2$, which we can fulfil by choosing T small enough (remember that $\delta\varphi^2_{\text{spnt}} \sim T/J_2$). In this way we have met all the biological constraints derived from the experiments and fixed all parameters of the ISM-FPUT model.

In Table I we present simulations of the ISM-FPUT model where we employed the procedure above starting from different values of J_2 separated by four orders of magnitudes; in all cases we can match every experimental condition: cohesion during the turn, Lorentzian correlation function, correct timescales. Considering that we left

TABLE I. Robustness of the ISM-FPUT scenario. There are four conditions that must be satisfied to have a biologically-plausible turn: the two dimensionless timescales of turn and relaxation, $\tau_{\text{turn}}/\tau_{\text{mot}}$ and $\tau_{\text{relax}}/\tau_{\text{mot}}$, must be matched to their experimental values, respectively, 28 and 2.6; the flock must remain cohesive during the turn; spontaneous fluctuations must have quasi-Lorentzian correlation. These last two conditions are granted as long as relation (B1) is satisfied, relation which we break up here into three separate inequalities: $\gamma_L^2/(J_4\delta\varphi^2_{\text{pert}}) \ll 1 - J_2/\gamma_L^2 \ll 1 - J_4\delta\varphi^2_{\text{spnt}}/J_2 \ll 1$. Starting from any value of J_2, we can chain-fix all other parameters in the Table, as described in Appendix B ($J_2 \to \eta \to v_0 \to \tau_{\text{turn}} \to J_4 \to T$). We do this for different values of J_2 spanning 4 orders of magnitude. In every simulation all biological requirements are met; in particular, because relation (B1) is satisfied in each instance, we always have cohesive turning (one connected component after the turn, $N_{\text{conn}} = 1$) and Lorentzian correlations of the spontaneous fluctuations. The case shown in Fig. 3 in the main text is ISM-FPUT 4.

	Simulation parameters						Biological constraints				
							$\tau_{\text{turn}}/\tau_{\text{mot}}$	$\tau_{\text{relax}}/\tau_{\text{mot}}$	$\gamma_L^2/J_4\delta\varphi^2_{\text{pert}}$	J_2/γ_L^2	$J_4\delta\varphi^2_{\text{spnt}}/J_2$
	J_2	η	v_0	τ_{turn}	J_4	T	28	2.6	$\ll 1$	$\ll 1$	$\ll 1$
ISM–FPUT 1	120	70	14	1.1	5.9×10^9	1.0×10^{-6}	27.9	2.7	1.2×10^{-3}	2.6×10^{-1}	2.5×10^{-2}
ISM–FPUT 2	59	70	5.5	2.9	2.9×10^7	5.0×10^{-5}	28.5	2.6	1.5×10^{-2}	1.3×10^{-1}	2.5×10^{-2}
ISM–FPUT 3	12	25	2.3	7.0	2.9×10^5	1.0×10^{-5}	28.2	2.5	3.2×10^{-2}	2.1×10^{-1}	1.3×10^{-3}
ISM–FPUT 4	1.18	7.0	1.04	16	5.9×10^4	1.0×10^{-6}	28.2	2.7	1.6×10^{-2}	2.6×10^{-1}	2.5×10^{-3}
ISM–FPUT 5	0.059	3.0	0.12	130	5.9×10^4	1.0×10^{-8}	27.6	2.6	2.1×10^{-2}	7.1×10^{-2}	1.0×10^{-2}
ISM–FPUT 6	0.012	0.70	0.12	130	5.9×10^3	1.0×10^{-8}	27.6	2.6	6.8×10^{-3}	2.6×10^{-1}	2.5×10^{-2}

completely arbitrary the values of $\{J_2, L, r_1, \chi, n_c\}$, we conclude that the reason why the new ISM-FPUT theory works is not a numerical fine-tuning of the parameters, but it is rather the freedom granted by decoupling the unperturbed dynamics (ruled by J_2), from the perturbed one (ruled by J_4).

A final comment is in order. The fact that $J_4\delta\varphi^2_{\rm pert}$ grows like the square root of J_4 (instead of linearly, as one may have naively guessed) have some peculiar consequences on the ratio between the quadratic and the quartic couplings. We recall that the procedure above requires that $\tau_{\rm turn} \sim J_2^{-1/2}$, which implies $J_4\delta\varphi^2_{\rm pert} \sim J_4^{1/2}\tau_{\rm turn}^{-1} \sim (J_2 J_4)^{1/2}$. Since the two terms J_2 and $J_4\delta\varphi^2_{\rm pert}$ in (B1) are separated by *two* asymptotic inequalities, if we allow 1 or 2 orders of magnitude for each inequality, we obtain $J_2 \sim 10^{-2}$–$10^{-4}(J_2J_4)^{1/2}$, that is $J_2 \sim 10^{-4}$–$10^{-8}J_4$. This fact explains why J_2 and J_4 end up differing by several orders of magnitude in the ISM-FPUT simulations (see Table I).

Appendix C: Excluding the overdamped hypothesis—In the main text we stated that the purely quadratic model ($J_4 = 0$) in the overdamped regime yields Lorentzian correlation, but it cannot produce biologically plausible turns. While this may seem completely obvious to some readers, there is also an intuition that if the quadratic alignment interaction J_2 is large enough, maybe turn propagation is attainable also in a purely quadratic overdamped model [46]. Having defined and measured the two dimensionless time scales (A1) to precisely characterize experimental turns, we can put this intuition to a quantitative test.

In order to compare different overdamped (OD) cases it is important to work at the same relative level of overdamping; to do this we require the smallest wave vector of the system, $k_{\rm min} = 2\pi/L$, to be equally overdamped in all cases at the level of linear response; we see from (4) that this requires the ratio $(J_2 n_c/\chi) r_1^2 k_{\rm min}^2/\gamma^2$ to be the same in all simulations and smaller than 1; remembering that $\gamma = \eta/2\chi$, we set $J_2 n_c 4\chi r_1^2 k_{\rm min}^2/\eta^2 = 0.26$. With this choice the correlation function of the overdamped cases is always Lorentzian, as discussed in the main text.

Table II lists various numerical attempts to achieve a turn by using a purely quadratic interaction ($J_4 = 0$), in the overdamped regime. The conclusion is that, although in this case it is indeed possible to make the flock turn without splitting ($N_{\rm conn} = 1$), as expected this can only be done by setting J_2 to a very large value, which however yields an unrealistically short relaxation time $\tau_{\rm relax}$, normalized to the motility time (OD2 case in Table II). We note that changing the temperature does not help in any way: as long as the system is in the highly ordered regime in which the linear spin-wave expansion (4) holds, the relaxation time in the overdamped case is independent of the temperature, $\tau_{\rm relax} = 2\eta/(J_2 n_c r_1^2 k^2)$, while the temperature merely enters as a prefactor (amplitude) of the correlation function. For example, if we run the same simulation as in OD2, but with $T = 10^{-4}$ instead of $T = 10^{-6}$, we get $\tau_{\rm relax}/\tau_{\rm mot} = 0.019$ (instead of 0.021), which is still completely different from the experimental value of 2.6 (this is OD5 in Table II).

To summarize, in absence of the quartic J_4 coupling, we have not found any combination of parameters that gives experimentally acceptable turns.

TABLE II. Excluding the overdamped (OD) hypothesis. We report here various failed attempts to obtain biologically plausible turns in the standard (i.e. $J_4 = 0$) overdamped ISM. Because overdamping will of course grant Lorentzian relaxation, the aim here would be to obtain $N_{\rm conn} = 1$ while keeping $\tau_{\rm relax}/\tau_{\rm mot}$ and $\tau_{\rm turn}/\tau_{\rm mot}$ close to the experimental values. Since the numerical parameter $\tau_{\rm turn}$ is independent of all other parameters of the simulation, we can always match $\tau_{\rm turn}/\tau_{\rm mot}$ to its experimental value. Instead, the relaxation time is a complex product of all parameters determining the dynamics; hence, matching $\tau_{\rm relax}/\tau_{\rm mot}$ while keeping cohesion is the real numerical challenge in reproducing the experimental data. In the overdamped (OD) regime, what typically happens is case OD1 [Fig. 1(c) in main text]: the flock splits and $\tau_{\rm relax}/\tau_{\rm mot}$ is much smaller than the experimental value. By increasing the alignment interaction coupling J_2, it is possible to obtain a collective turn without splitting the flock (OD2), but $\tau_{\rm relax}/\tau_{\rm mot}$ drops to 2 orders of magnitude below the experimental value. Attempting to fix $\tau_{\rm relax}/\tau_{\rm mot}$ through v_0 (which changes $\tau_{\rm mot}$ and requires a corresponding change in $\tau_{\rm turn}$), as in OD3 and OD4, results in splitting, both with small and large values of J_2. Changing the temperature with respect to OD2 does not improve the situation (OD5). As a matter of fact, there is no way to obtain a biologically plausible turn in the overdamped phase of a purely quadratic model. The case shown in the main text is ISM-FPUT 4.

	Simulation parameters				Biological constraints					
					$N_{\rm conn}$		$\tau_{\rm turn}/\tau_{\rm mot}$		$\tau_{\rm relax}/\tau_{\rm mot}$	
	J_2	η	v_0	T	1		28		2.6	
OD1	1.18	7	0.1	10^{-6}	2	✗	28.1	✓	0.29	✗
OD2	294	112	0.1	10^{-6}	1	✓	28.1	✓	0.021	✗
OD3	1.18	7	1.04	10^{-6}	2	✗	28.1	✓	2.7	✓
OD4	294	112	12	10^{-6}	2	✗	28.2	✓	2.5	✓
OD5	294	112	0.1	10^{-4}	2	✗	28.1	✓	0.019	✗